Graphene at fluidic interfaces

Belyaeva, L.A.

CHAPTER 5

Hydrophilicity of graphene in water through transparency to polar and dispersive interactions

Establishing contact angles on graphene-on-water has been a long-standing challenge as droplet deposition causes free-floating graphene to rupture. In this chapter ice and hydrogels are used as substrates mimicking water while offering a stable support for graphene. The lowest water contact angles of graphene were measured, namely on graphene-on-ice and graphene-on-hydrogel. The contact angle measurements of liquids with a range of polarities allowed to quantify the transparency of graphene towards polar and dispersive interactions demonstrating that graphene in water is hydrophilic. These findings are anticipated to shed light on the inconsistencies reported so far on the wetting properties of graphene, and most particularly on their implications towards rationalizing how molecules interact with graphene in water.

This chapter was published as an article: Liubov A. Belyaeva, Pauline M.G. van Deursen, Kassandra I. Barbetsea, Grégory F. Schneider Adv. Mater. 2018, 30, 1703274

5.1. Introduction

The wetting properties of graphene are more complicated than those found in regular solid-liquid interfaces because graphene possesses no bulk phase and is only composed of a single atomic layer of carbon atoms separating two liquid media. Graphene is therefore subjected to a complexity of nonspecific interactions with adsorbates – primarily induced by wetting transparency – at the substrate-graphene-liquid and liquid-graphene-liquid interfaces.[1]

Wetting transparency, opacity, hydrophilicity and hydrophobicity of graphene remain under debate. Intensive recent studies on the wetting transparency of graphene suggested that the wettability of graphene is governed by the wettability of the underlying support.[1–3] Other studies report complete wetting transparency of graphene when deposited on gold, copper and silicon, but not glass, where interactions with water are considered short-range[2]. A later experimental work supported by molecular dynamics simulations suggests partial transparency of graphene and indicates that wetting transparency does not occur for superhydrophilic or superhydrophobic substrates,[3] and number of papers suggest full wetting opacity of monolayer graphene irrespective of the substrate, with contact angle values similar to water contact angle on graphite.[4–6] Consequently, contact angle values of water on graphene vary from 33° for graphene on silicon[2] to 90-127° for graphene respectively on silicon carbide, silicon oxide and copper[4–7] despite a large number of theoretical studies suggesting that water contact angle values on graphene should be similar to the one of graphite.[1,4,6] So far, the several contradictions and inconsistencies have partially been explained by the presence of adsorbates, graphene defects and surface charges.[8,9]

Concerning the wetting properties of graphene in water, the direct measurement of the contact angle of water on graphene-on-water – i.e., depositing a droplet of water on graphene floating on water – has been technically impossible due to the immediate rupture of the graphene upon droplet deposition (Figure 5.1a, b) resulting from the growth- and handling-induced cracks and tears.[10–13] Probing wetting properties of graphene in water and water solutions is, however, particularly important for application in sensing, water filtration, fuel cell membranes and more generally when graphene is exposed to water from the

both sides.[1,14–16] This chapter shows that graphene is surprisingly hydrophilic when floating on water. Additionally, by changing the polarity of the liquid used to measure contact angles (both of the drop and of the solution), the surface energy of graphene was calculated indicating that monolayer graphene is transparent to both polar and dispersive interactions – i.e. fully transparent to wetting – with the condition that a smooth substrate/graphene/liquid interface free of contamination is obtained. In the contrary case – that is when graphene is physically transferred from the growth substrate to another support – graphene usually does not conform perfectly the target substrate resulting in the screening of short-range polar interactions while long-range dispersion interactions are fully transmitted. The latter often occurs in scenarios where graphene is transferred with the use of a polymer yielding surface corrugations, wrinkles, contamination, large sample-to-sample variations and immense discrepancies in the contact angles measurements.

5.2. Results and discussions

To quantify the hydrophobicity of graphene and to rationalize its wetting properties, ice and hydrogels can be used as models of liquid water. In fact, the water molecules at the surface of ice are in a supercooled liquid state retaining an amorphous liquid-like structure.[17–21] Separately, a low weight percent hydrogel has a low surface concentration of polymer chains relative to that of interstitial water and, for that reason, has been used as a quasi-solid model for water surface properties since the sixties.[22,23] By experimentally measuring the contact angle of water on floating graphene, the lowest contact angle reported for graphene so far were observed: 30±5° on ice and 10±2° on a 4 w% agarose hydrogel.

Importantly, the cleanliness of the graphene surface and of the graphene-substrate interface are critical factors for a reliable contact angle measurement and great care should be taken for the handling of graphene. For details on the cleaning procedure (e.g. from polymer residuals or hydrocarbon adsorbates), including handling and control measurements, see Appendix 4.

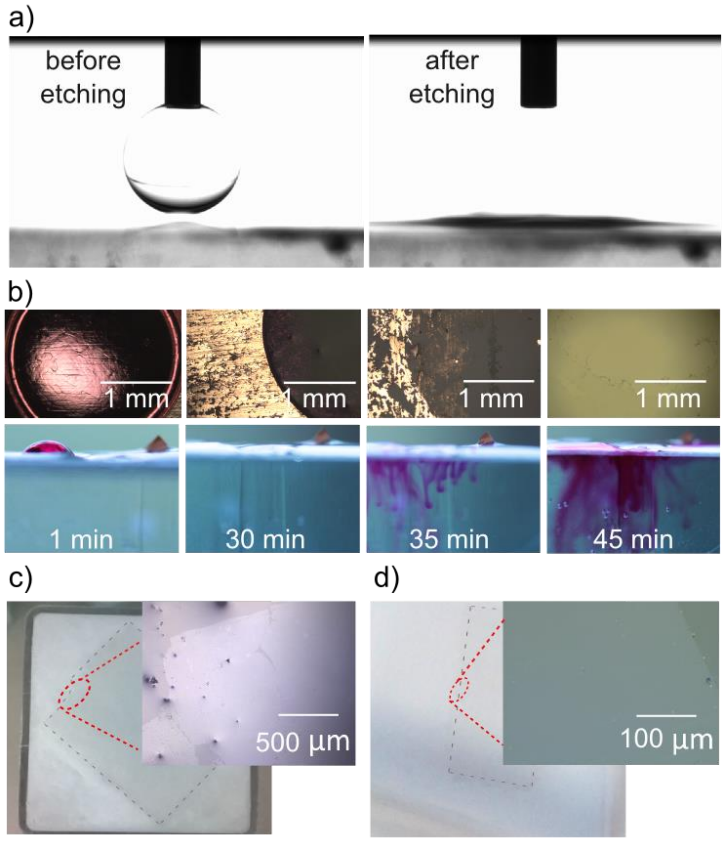

Figure 5.1. **Graphene free-floating on liquid water, ice and hydrogels.** a) Water contact angle (WCA) measurements of graphene floating on a water surface. Left: water droplet before being deposited on the surface of CVD-graphene floating on an aqueous solution of copper etchant. Right: a water droplet after being deposited on the surface of graphene sinks through the graphene, preventing the measurement of the contact angle. The rupture and consequent breaking of the graphene is also seen in the case of pure water instead of APS solution. b) Time lapse photographs of a water droplet sinking through a graphene/copper stack floating on the surface of an aqueous solution of ammonium persulfate (copper etchant) as a function of copper etching time (from left to right). Photographs were taken from the top of the droplet (top images) and from the side (bottom images). The water droplet was dyed with Rhodamine B for optimal visualization. c) Photograph and optical microscopy image (inset) of a monolayer of graphene on ice. d) Photograph and optical microscopy image (inset) of a monolayer of graphene on a 4% agarose hydrogel.

5.2.1. Graphene is hydrophilic in an aqueous environment

Investigating the wetting properties of graphene suspended on a liquid poses a critical challenge: although intact graphene floats well on water – presenting a graphene-on-water surface – the contact angle of such a surface cannot be measured (and has never been measured) because free-floating graphene immediately breaks apart when a droplet of water is casted onto the graphene top surface, inducing excessive mechanical and interfacial stress resulting in cracking and tearing of graphene, causing the water to leak out via the formed microcracks (Figure 5.1a). Those microcracks might result from the growth,[10,11,13] during copper etching[10–12] or simply under the droplet pressure. The water droplet therefore sinks through graphene even if the droplet is deposited before copper is completely etched away, i.e. when the dynamic stress in graphene is minimized (Figure 5.1b). To overcome this limitation and to probe the wetting properties of graphene in water, liquid water underneath graphene was replaced with water ice and an agarose hydrogel (Figure 5.1c and 5.1d). These systems are especially benign to graphene as they avoid using a protective polymer (usually PMMA) layer that always yields contamination such as polymer residues.

5.2.2. Ice as a model for water

Graphene grown by CVD on copper (see Methods for details) is placed on the surface of an aqueous solution of 0.5 M ammonium persulfate (APS), which serves as a copper etchant. After cool-down and the solidification of water, the contact angle of a droplet of water deposited on graphene-on-ice was measured. To prevent condensation, the chamber was flushed with dry air during the entire process of water freezing and measurements. Another possible source of inaccuracy in measurements is strain in graphene that may be induced upon freezing of water. However, later in this chapter it will be shown that it does not affect the wetting transparency, as in the case of strain no significant change in graphene-ice distance occurs to screen the interactions. The contact angle and surface energy of graphene on ice were found to be very close to those of bare ice.

Remarkably, the water contact angle (WCA) on graphene-on-ice at 0°C is 30°±5 which is only 13° greater than the water contact angle of pure ice and 30° smaller than the water contact angle of freshly exfoliated graphite (see Figure 5.2a). Repeating the experiment with double layer graphene increases the WCA to 35° on average. At -20°C the WCA also showed a similar hydrophilic behavior of graphene when deposited on ice (see Figure 5.2a). To prevent the water droplet from instant freezing at the moment of its deposition on graphene, 18% of nitric acid was added (see Methods in Appendix 4), yielding slightly smaller contact angles compared to experiments carried at 0°C due to the increase in the polarity of the liquid droplet: 11°±3 for ice, 18°±4 for monolayer graphene on ice, 34°±5 for bilayer graphene on ice and 57°±2 for graphite. To take into consideration the effect of added nitric acid on the contact angle and on the surface energy the approach typically used for an electrolyte solution was followed (experimental details and calculations of the surface energy can be found in Appendix 4). One and two layers of graphene, therefore, transmit major portion of water-water interactions, although the bilayer is less hydrophilic and screens a noticeable part of the interactions due to the increased thickness.

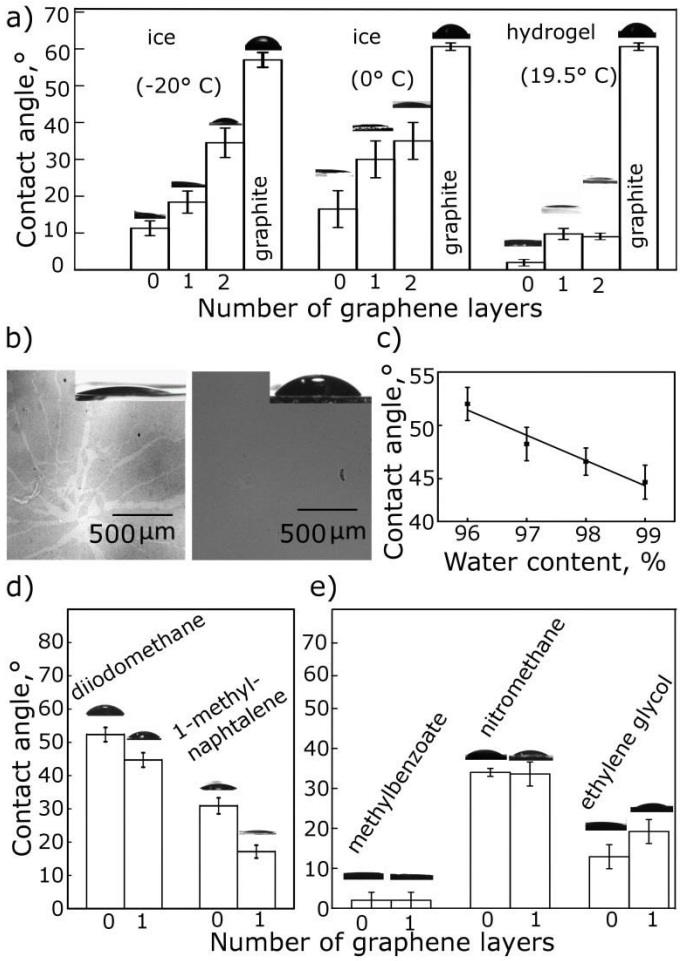

Figure 5.2. Contact angles of graphene on ice and hydrogel. a) Water contact angle (WCA) of graphene-on-ice measured at -20°C, 0°C and for graphene on a 4% agarose hydrogel measured at 19.5°C. WCA were measured for bare ice/hydrogel, monolayer graphene and bilayer graphene. b) Contact angle photographs (insets) and optical microscopy images of the graphene after drop-casting water (left) and diiodomethane (right) on top of graphene floating on a 4% agarose hydrogel. The process of drop-casting a droplet of water typically causes graphene to crack while drop-casting of an organic liquid leaves no visible mechanical damages on graphene. c) Hydrogel as a water model: diiodomethane contact angle values for an agarose hydrogel with different water content. d) Contact angles of graphene on a 4% agarose hydrogel with diiodomethane and 1-methylnaphtalene as liquid droplets. e) Contact angle values of graphene on ice with methylbenzoate, nitromethane and ethylene glycol.

Although the properties of ice differ from the properties of liquid water, the surface of ice stays in a supercool state and retain amorphous liquid-like structure,[17–21] which makes ice with graphene on top a reasonable approximation of free-floating graphene on water.

5.2.3. Hydrogel as a model of water

In the graphene-hydrogel system developed for contact angle measurements, CVD graphene grown on copper was supported by a 4% agarose gel network.[24]

Graphene on hydrogel is hydrophilic, with a contact angle of 10±2° for single layer graphene. Optical microscopy images of graphene on hydrogel after contact angle measurement with water (left) and diiodomethane (right) are shown in Figure 5.2b. The micrographs show that multiple cracks have formed after the deposition of a water droplet (Figure 5.2b, left) while an intact surface is preserved during the deposition of organic liquids (Figure 5.2b, right). The cracking under the influence of water is attributed to the strong interactions between water underneath graphene and water in the droplet. Despite the appearance of cracks, no water leaks away into the gel, as water droplets attain a stable shape within three seconds after drop deposition – during which the droplet spreads out. Moreover, the graphene coverage, despite the presence of cracks, was still well above 95%, with no noticeable cracks on the periphery of the droplet. Analogous crack analysis was not possible for ice samples due to technical limitations: because the sample has to be cooled down the liquid droplet does not evaporate after the contact angle measurement, rendering impossible to inspect the surface of ice using a microscope.

By measuring contact angles of water-immiscible solvents on hydrogels with a range of agarose concentrations, a linear extrapolation was made to 100% water.[22] Figure 5.2c shows the linear extrapolation of the contact angle of diiodomethane on an agarose hydrogel with agarose concentrations range from 1 to 4% agarose in weight (see Figure A4.7 in Appendix 4 for the extrapolation with 1-methylnaphtalene). From the extrapolation, the contact angle of diiodomethane on water would be 41°. Conversely, such data cannot be gathered

for graphene-on-hydrogel, because graphene relies on a high (4%) agarose concentration for mechanical support.

In summary, two independent experiments have proven that when placed in a water-like environment, graphene, surprisingly, presents hydrophilic properties very close to those of pure water, i.e. graphene is transparent to water-water interactions. Studying only graphene-water interactions, however, is not sufficient for understanding graphene wetting properties and claiming its wetting transparency.

For that reason contact angle measurements with other liquids possessing different polarities were performed (Table A4.1 in Appendix 4). With all probed liquids, graphene-on-ice and graphene-on-hydrogel showed contact angle similar to the contact angles on pure ice and pure hydrogel respectively (Figure 5.2d and e). Contact angles with organic liquids seem to be more reliable than those with water, as no damage to the graphene structure occurs during the measurement (see Figure 5.2b for comparison). The damage that typically occurs for measurements with water can result from very strong water-water interactions between the water molecules across the graphene sheet.

5.2.4. Selective screening of polar interactions by graphene: Is graphene transparent to wetting?

To explain the inconsistencies reported in literature on the contact angle of graphene, it is logical to question whether the great variety of WCA reported for graphene results from the fact that graphene transmits only a part of the interactions between the substrate and the liquid. In that case, transparency or opacity of graphene to wetting would be determined by the dominating type of interactions between the molecules constituting the droplet and the substrate, and its transmission through a graphene layer. Depending on the chemical nature of the adsorbate and adsorbent, all intermolecular interactions can be divided into two main groups: site-specific *polar* (hydrogen bonding, dipole-dipole, and dipole-induced interactions) and nonspecific *dispersive* interactions (London - van der Waals interactions)[25,26]. Polar interactions appear whenever the electron density or a positive charge are localized along the bonds; and dispersive

interactions appear due to instantaneous dipole moments of all atoms and molecules and, therefore, are always present regardless of the chemical nature of the interacting molecules. These two types of interactions can be quantified in terms of surface energy components.[26,27] According to the Owens-Wendt[26] or Fowkes[22] theory, the total surface tension of a liquid or a solid can be represented as a sum of polar and dispersive components corresponding to polar and dispersive interactions:

$$\sigma_L = \sigma_L^P + \sigma_L^D$$
$$\sigma_S = \sigma_S^P + \sigma_S^D$$

and all four components can be linked with each other by the Owens-Wendt equation:

$$\frac{\sigma_L(cos\theta + 1)}{2\sqrt{\sigma_L^D}} = \frac{\sqrt{\sigma_S^P}\sqrt{\sigma_L^P}}{\sqrt{\sigma_L^D}} + \sqrt{\sigma_S^D}$$

Calculating the surface energies using the Fowkes model[22,27] yielded a good agreement with the surface energies obtained using the Owens-Wendt model (see Figure A4.12 in Appendix 4). Detailed calculations of surface energies by Owens-Wendt theory and results of the Fowkes calculations can be found in Appendix 4.

Probing contact angles of liquids with different polarities allowed to determine polar σ_S^P and dispersive σ_S^D components of the solid and to identify the character of the interactions between the droplet and the solid.[26] The variation of the σ_S^P and σ_S^D caused by the addition of the graphene layer was examined in order to elucidate what interactions are transmitted or screened by the graphene and to what extent. Water, diiodomethane and 1-methylnaphthalene were chosen because of their compatibility with the hydrogel matrix. Their polar and dispersive components are tabulated (see Table A4.1 in Appendix 4). More in details: water, methyl benzoate, nitromethane and ethylene glycol were chosen as test liquids for ice due to their low freezing points and known polar and dispersive components; and water, diiodomethane, formamide, nitromethane and methyl benzoate were chosen for Si/SiO_2, polydimethylsiloxane (PDMS) and copper (Table A4.1 in Appendix 4).

Separately, three types of substrates possessing three distinct surface free energies were chosen: substrates with dominating polar component (i.e., ice and hydrogel), substrates with similar polar and dispersive components (i.e., Si/SiO_2 wafers and PDMS), and a substrate with dominating dispersive component (i.e., copper). Importantly, because graphene has not been transferred on copper, ice and hydrogel (see Methods for the details on the samples preparation), graphene conforms the surface of the substrates allowing for a perfect adhesion.[28] Contrarily, graphene being transferred from copper does not conform as effectively the PDMS surface and possesses multiple out-of-plane irregularities such as wrinkles, bucklings and foldings,[29,30] resulting in a larger graphene-substrate separation and, consequently, poorer adhesion.[28]

As shown in Figure 5.2, graphene does not alter contact angles of all tested liquids when deposited on top of copper, ice or hydrogel and, consequently, transmits both polar and dispersive interactions (Figure 5.3). Important to note, that an increase in the number of graphene layers results in poorer reproducibility due to contamination, defect formation, and uncontrollable interlayer distance occurring during the transfer of the layers on top of each other (the multilayer samples were purchased from Graphenea, and are prepared prepare by repetitively transferring graphene layers on top of each other). The error margins are therefore wider for bilayer graphene than those for monolayer graphene, and error margins for three- and four- layer graphene did not allow making a conclusion on the average contact angle value (see Figure A4.9 in Appendix 4). Importantly, in all cases graphene showed contact angles different from the contact angle of freshly-exfoliated (to avoid airborne hydrocarbons contamination) graphite measured to be 61±3° which is consistent with previously reported values.[8,31–33]

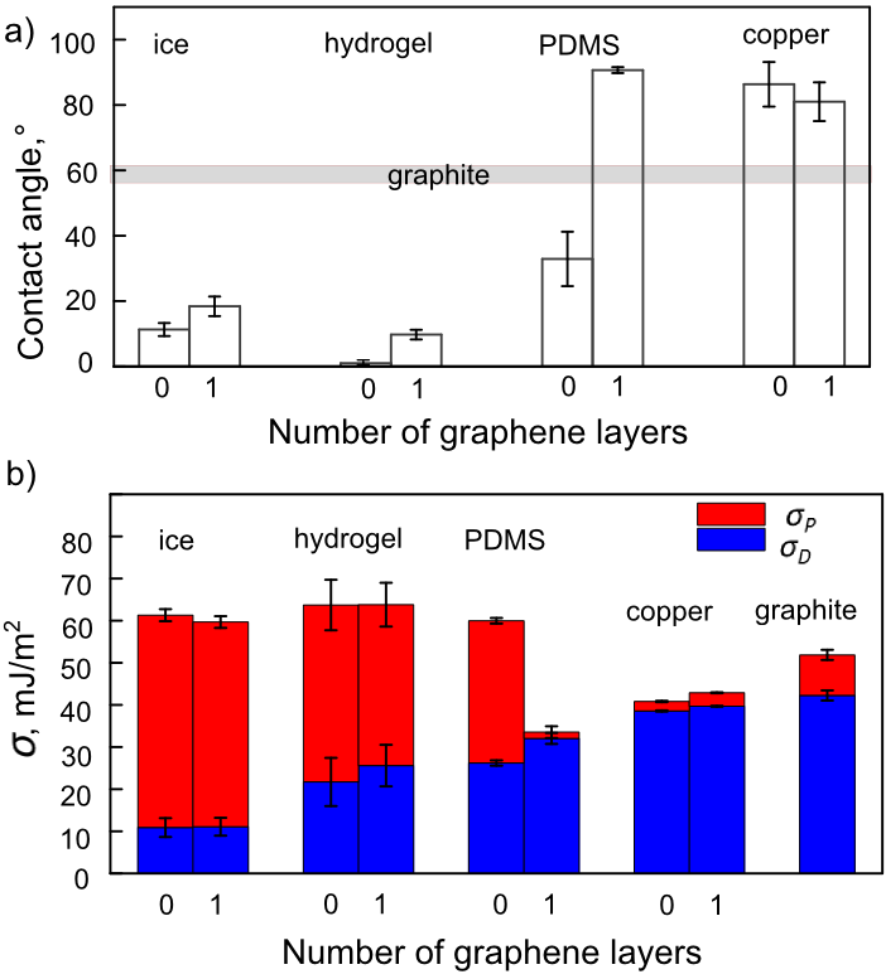

Figure 5.3. Water contact angle values and surface energy of graphene on different substrates compared to bare substrates. a) Water contact angle (WCA) of graphene deposited on ice (-20°C), hydrogel (19.5°C), PDMS (19.5°C) and copper (19.5°C) versus WCA of pristine ice, hydrogel, PDMS and copper. b) Polar and dispersive components of the surface energy of graphene deposited on ice, hydrogel, PDMS and copper versus pristine ice, hydrogel, PDMS and copper. The polar and dispersive components of the surface energy were calculated using the Owens-Wendt theory.

The transparency effect for ice, hydrogel and copper is even more evident from the surface energy chart (Figure 5.3b). Surface energy calculations are based on the contact angle measurements with various liquids and are, in that respect, a

more comprehensive characteristic of the interactions than a contact angle measurement. Notably, the total surface energy of graphene supported by a substrate is different from the total surface energy of graphite (52±2 mJ/m^2) for all tested substrates and equals to the surface energy of the bare substrate itself with the only exception of PDMS, as shown in Figure 5.3b (~60 mJ/m^2 for ice, ~64 mJ/m^2 for hydrogel and ~43 mJ/m^2 for copper). Thus, although graphene is often considered as a graphite-like material and expected to have graphite-like wetting behavior and surface energy,[5,7,8] clearly, its surface energy and wetting properties are governed by the bulk medium underneath. Furthermore, the presence of graphene does not affect the distribution of polar and dispersive forces between the molecules of adsorbate and adsorbent for all types of substrates (the case of PDMS will be discussed further below). Noteworthy, surface energies and polar and dispersive components of the surface energies of ice, graphene-on-ice, hydrogel and graphene-on-hydrogel are all very close to those of pure water, which indicates that ice and hydrogels are suitable as water models for probing wetting properties of graphene in water.

As opposed to graphene-on-ice, graphene-on-hydrogel or graphene-on-copper, graphene transferred onto a Si/SiO_2 wafer or onto a PDMS slab showed significantly different wetting properties than the substrate underneath it (Figure 5.3a and Figure A4.10 in Appendix 4). Moreover, measurements for graphene on Si/SiO_2 (but not for bare Si/SiO_2 wafers, which were reproducible) were highly irreproducible with all tested liquids with water contact angles varying from 40° to 90° (Figure A4.10 in Appendix 4) and were therefore not included in the present analysis. This can be attributed to the different graphene-substrate adhesion forces that result from sample-to-sample variation occurring during the transfer process. Although electronic properties of graphene on Si/SiO_2 are well defined in literature, contamination and even subtle alterations of adhesion forces - which have minor effects on the electronic properties - can crucially affect the wetting properties of graphene.

Transfer of graphene to PDMS is more straightforward and, importantly, does not involve coverage of graphene with another polymer than PDMS, permitting reproducible contact angle measurements (see Methods in Appendix 4 for more details on the transfer). After transferring graphene onto PDMS the water contact angle increased from 33±5° to 91±1° (see Figure 5.3a) and the total

surface energy decreased from 60±1 mJ/m^2 to 34±1 mJ/m^2 (Figure 5.3b). The polar component dropped drastically from 34±1 mJ/m^2 to 2±1 mJ/m^2, whereas the dispersive component remained almost unchanged at 26±1 mJ/m^2. Given the full transparency of graphene to the both types of interactions for "well-conforming" substrates, the selective screening of the polar interactions therefore originates from the mismatch in conformation between the surface of graphene and PDMS caused by the transfer process. The lack of conformity between a substrate and graphene transferred on top of it has been independently proven by the AFM analysis of the surface morphology of PDMS with and without graphene (Figure A4.2 in Appendix 4). Graphene transferred to PDMS rather represents the roughness pattern of copper than of PDMS which results in conformational mismatch and breakdown of the wetting transparency of graphene (Figure A4.2 in Appendix 4). Polar interactions are short-range and, therefore, evanesce upon increasing the adsorbate-adsorbent distance whereas long-range dispersion interactions can still be fully transmitted.[34–37] This implies that the observed polar component of 2±1 mJ/m^2 can be attributed to the inherent polar component of graphene.

Noteworthy, to exclude the influence of adsorbed contaminants from air,[8] samples of graphene on copper and Si/SiO_2 were annealed before the measurements (see Appendix 4 for more details).

5.3. Conclusions

The mechanical fragility of a single layer of graphene floating on the surface of water has prevented so far to probe the surface hydrophilicity by means of contact angle measurements. Contact angle measurements of graphene on water ice and on hydrogels show that graphene is hydrophilic and transparent to water-water interactions. Importantly, the interface between the graphene layer and underlying substrate plays an important role: graphene transmits polar and dispersive interactions if the graphene-substrate interface is clean and not corrugated, otherwise polar interactions are screened while dispersive interactions are transmitted. In applications where graphene is suspended between two liquids, these results now shed light and propose a radically

different understanding of the wetting properties of graphene and will have prompt implications in understanding how hydrophobic and hydrophilic molecules interact with the surface of a two-dimensional material subjected to full wetting transparency. This work might also inspire several research communities to (re)consider how hydrophilicity and hydrophobicity of two-dimensional materials and molecules are defined.

5.4. References

1. Driskill, J., Vanzo, D., Bratko, D. & Luzar, A. Wetting transparency of graphene in water. *J. Chem. Phys.* **141,** 18C517 (2014).

2. Rafiee, J. *et al.* Wetting transparency of graphene. *Nat. Mater.* **11,** 217–222 (2012).

3. Shih, C. J. *et al.* Breakdown in the wetting transparency of graphene. *Phys. Rev. Lett.* **109,** 1–5 (2012).

4. Taherian, F., Marcon, V., Van Der Vegt, N. F. A. & Leroy, F. What is the contact angle of water on graphene? *Langmuir* **29,** 1457–1465 (2013).

5. Shin, Y. J. *et al.* Surface-energy engineering of graphene. *Langmuir* **26,** 3798–3802 (2010).

6. Raj, R., Maroo, S. C. & Wang, E. N. Wettability of graphene. *Nano Lett.* **13,** 1509–1515 (2013).

7. Wang, S., Zhang, Y., Abidi, N. & Cabrales, L. Wettability and surface free energy of graphene films. *Langmuir* **25,** 11078–11081 (2009).

8. Li, Z. *et al.* Effect of airborne contaminants on the wettability of supported graphene and graphite. *Nat. Mater.* **12,** 925–931 (2013).

9. Ghaderi, N. & Peressi, M. First-principle study of hydroxyl functional groups on pristine, defected graphene, and graphene epoxide. *J. Phys. Chem. C* **114,** 21625–21630 (2010).

10. Arjmandi-Tash, H., Jiang, L. & Schneider, G. F. Rupture index: A quantitative measure of sub-micrometer cracks in graphene. *Carbon N. Y.* **118,** 556–560 (2017).

11. Belyaeva, L. A., Fu, W., Arjmandi-Tash, H. & Schneider, G. F. Molecular caging of graphene with cyclohexane: transfer and electrical transport. *ACS Cent. Sci.* **2,** 904–909 (2016).

12. Gao, L. *et al.* Face-to-face transfer of wafer-scale graphene films. *Nature* **505,** 190–194 (2014).

13. Hwangbo, Y. *et al.* Fracture characteristics of monolayer CVD-graphene. *Sci. Rep.* **4,** 4439 (2015).

14. Postma, H. W. C. Rapid sequencing of individual DNA molecules in graphene nanogaps. *Nano Lett.* **10,** 420–425 (2010).

15. Arjmandi-Tash, H., Belyaeva, L. A. & Schneider, G. F. Single molecule detection with graphene and other two-dimensional materials: nanopores and beyond. *Chem. Soc. Rev.* **45,** 476–493 (2016).

16. Cohen-Tanugi, D. & Grossman, J. C. Water desalination across nanoporous graphene. *Nano Lett.* **12,** 3602–3608 (2012).

17. Faraday, M. On certain conditions of freezing water. *Athenaeum* 283–284 (1850).

18. Elbaum, M., Lipson, S. G. & Dash, J. G. Optical study of surface melting on ice. *J. Cryst. Growth* **129,** 491–505 (1993).

19. Kuroda, T. & Lacmann, R. Growth kinetics of ice from the vapour phase and its growth forms. *J. Cryst. Growth* **56,** 189–205 (1982).

20. Jellinek, H. H. . Adhesive properties of ice. *J. Colloid Sci.* **14,** 268–280 (1959).

21. Asakawa, H., Sazaki, G., Nagashima, K., Nakatsubo, S. & Furukawa, Y. Two types of quasi-liquid layers on ice crystals are formed kinetically. *Proc. Natl. Acad. Sci.* **113,** 1749–1753 (2016).

22. Van Oss, C. J., Roberts, M. J., Good, R. J. & Chaudhury, M. K. Determination of the apolar component of the surface tension of water by contact angle measurements on gels. *Colloids and Surfaces* **23,** 369–373 (1987).

23. Van Oss, C. J., Ju, L., Chaudhury, M. K. & Good, R. J. Estimation of the polar parameters of the surface tension of liquids by contact angle measurements on gels. *J. Colloid Interface Sci.* **128,** 313–319 (1989).

24. Zhang, D. *et al.* The electrochemical transfer of CVD-graphene using agarose gel as solid electrolyte and. *Chem. Commun.* **51,** 2987–2990 (2015).

25. Kiselev, A. V. Non-specific and specific interactions of molecules of different electronic structures with solid surfaces. *Discuss. FARADAY Soc.* 205–218 (1965).

26. Owens, D. K. & Wendt, R. C. Estimation of the surface free energy of polymers. *J. Appl. Polym. Sci.* **13,** 1741–1747 (1969).

27. Fowkes, F. M. Attractive forces at interfaces. *Ind. Eng. Chem.* **56,** 40–52 (1964).

28. Yoon, T. *et al.* Direct measurement of adhesion energy of monolayer graphene as-grown on copper and its application to renewable transfer process. *Nano Lett.* **12,** 1448–1452 (2012).

29. Deng, S. & Berry, V. Wrinkled, rippled and crumpled graphene: An overview of formation mechanism, electronic properties, and applications. *Mater. Today* **19,** 197–212 (2016).

30. Tang, X., Xu, S., Zhang, J. & Wang, X. Five orders of magnitude reduction in energy coupling across corrugated graphene / substrate interfaces. *ACS Appl. Mater. Interfaces* **6,** 2809–2818 (2014).

31. Tadros, M. E., Hu, P. & Adamson, A. W. Adsorption and contact angle studies I. Water on smooth carbon, linear polyethylene, and stearic acid-coated copper. *J. Colloid Interface Sci.* **72,** 515–523 (1979).

32. Kozbial, A., Trouba, C., Liu, H. & Li, L. Characterization of the intrinsic water wettability of graphite using contact angle measurements: Effect of defects on static and dynamic contact angles. *Langmuir* **33,** 959–967 (2017).

33. Ondarçuhu, T. *et al.* Wettability of partially suspended graphene. *Sci. Rep.* **6,** 24237 (2016).

34. Buckingham, a. D. Theory of long-range dispersion forces. *Discuss. Faraday Soc.* **40,** 232 (1965).

35. Leite, F. L., Bueno, C. C., Da Róz, A. L., Ziemath, E. C. & Oliveira, O. N. Theoretical models for surface forces and adhesion and their measurement using atomic force microscopy. *Int. J. Mol. Sci.* **13,** 12773–12856 (2012).

36. Hamaker, H. C. The London-Van Der Waals attraction between spherical particles. *Physica* **4,** 1058–1072 (1937).

37. Tai Yup Chang. Moderately long-range interatomic forces. *Rev. Mod. Phys.* **39,** 911–942 (1967).